the
abdus salam
international
centre
for theoretical
physics

united nations educational, scientific and cultural organization

international atomic energy agency

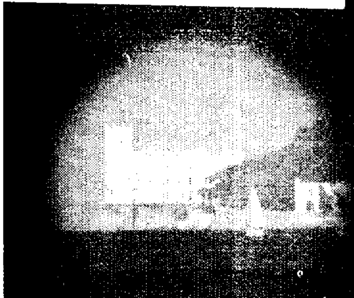

preprint

STARK EFFECT OF EXCITONS IN CORRUGATED LATERAL SURFACE SUPERLATTICES: EFFECT OF CENTRE-OF-MASS QUANTIZATION

Hong Sun

Available at: http://www.ictp.trieste.it/~pub_off IC/98/215

United Nations Educational Scientific and Cultural Organization
and
International Atomic Energy Agency
THE ABDUS SALAM INTERNATIONAL CENTRE FOR THEORETICAL PHYSICS

STARK EFFECT OF EXCITONS IN CORRUGATED LATERAL SURFACE SUPERLATTICES: EFFECT OF CENTRE-OF-MASS QUANTIZATION

Hong Sun
Department of Physics, Shanghai Jiao Tong University,
Shanghai 200030, People's Republic of China,[1]
Department of Physics, The Chinese University of Hong Kong,
Shatin, NT, Hong Kong
and
The Abdus Salam International Centre for Theoretical Physics, Trieste, Italy.

Abstract

The quantum confined Stark effect (QCSE) of excitons in GaAs/AlAs corrugated lateral surface superlattices (CLSSLs) is calculated. Blue and red shifts in the exciton energies are predicted for the heavy- and light-excitons in the CLSSLs, respectively, comparing with those in the unmodulated quantum well due to the different effective hole masses in the parallel direction. Sensitive dependence of the QCSE on the hole effective mass in the parallel direction is expected because of the "centre-of-mass" quantization (CMQ) induced by the periodic corrugated interfaces of the CLSSLs. The effect of the CMQ on the exciton mini-bands and the localization of the excitons in the CLSSLs is discussed.

MIRAMARE – TRIESTE
November 1998

[1]E-mail: shong@mail.sjtu.edu.cn

1. Introduction:

Ever since the discovery of the large quantum-confined Stark effect (QCSE) in quantum wells[1], modulations of absorption coefficients and refraction indexes in low dimensional electronic systems by external electric fields have attracted a great deal of attention for its potential device applications in designing high-speed, low-driving voltage optical modulators, switches and detectors. The QCSE in InAlGaAs/InGaAs and InAsP/GaInP multi-quantum wells (QWs) has been used to design high-speed, high-efficiency optical modulators operating near 1.06, 1.3 and 1.55μm wavelengths,[2–4] which have important applications in long-distance optical fiber communications. Voltage-tunable infrared photodetectors making use of the large Stark shifts of the strong intersubband absorptions in coupled QWs have been proposed[5]. And very recently, waveguide modulators based on the QCSE in II–VI semiconductor multi-QWs were fabricated,[6–8] motivated by their potential for monolithic integration with room-temperature II–VI semiconductor lasers operating in the blue/green spectral region. Investigations on the QCSE in different low dimensional systems, such as quantum wires[9] and dots[10], are being carried out in searching for systems with more adjustable parameters to control the QCSE according to one's needs.

Rapid advances in modern microstructure technology has made it possible to fabricate two dimensional (2D) electron systems with additional periodic modulations along their lateral directions. Structures with short lateral periods ($\sim 10nm$) comparable to the vertical dimension of these 2D systems have been produced by direct crystal growth methods, which include (i) deposition of GaAs and AlAs fractional layers on (001) GaAs vicinal surfaces[11]; (ii) direct molecular-beam epitaxy growth of GaAs and AlAs layers on high-index GaAs surfaces[12]; and (iii) direct molecular-beam epitaxy growth of (GaAs) quantum wells on cleaved facets of (GaAs/AlAs) superlattices[13], etc. These structures are often referred to as corrugated lateral surface superlattices (CLSSLs), since the lateral modulations arise from the corrugated interfaces separating the well and barrier materials of the systems. The dimension of the CLSSLs is between the 2D QWs and 1D quantum wires. Their lateral periods and corrugated interfaces offer additional adjustable parameters for one to control the QCSE according to one's application requirements. The periodic corrugated interfaces of the CLSSLs not only affect the internal motion of the exciton by confining the electron and hole into "wires", but also quantize the motion of its center-of-mass (CM) in the lateral directions. Theoretical studies on excitons in similar systems have been reported in the literature.[14,15] The effect of the "centre-of-mass" quantization (CMQ) of the excitons by the lateral periodic potential of the systems was considered in some of these reports[14]. It was pointed out there that unlike in the QW case, where 2D excitons can transfer from the CMQ to the "size" quantization, the latter is impossible in the CLSSLs with the lateral directions due to the unlimited binding energy of 1D excitons. The effect of the CMQ must be considered in the calculation of the exciton states in the CLSSLs. When electric fields are applied vertically to the CLSSLs, apart from changing the internal motion of the excitons by pulling the electron and hole apart, the electric fields also change the CMQ of the excitons by shifting the excitons towards or away from the corrugated interfaces. The exciton energies in the CLSSLs change with the applied electric fields in a complicated way. In this paper, we present the results of a model calculation of the exciton QCSE in the GaAs/AlAs CLSSLs.

2. Formulation:

The CLSSL model is the same as that we considered in a previous paper[16] with only one of its interfaces being corrugated, which resembles the CLSSL fabricated by deposition of GaAs and AlAs fractional layers on (001) GaAs vicinal surfaces[11]. Recent cyclotron resonance experiments on the system showed significant deviations of the cyclotron energy from what is expected in an unmodulated 2D electron system[17]. The novel behavior has been attributed to the cyclotron-resonance-intersubband coupling induced by the corrugated interfaces of the CLSSLs. Considering the intermixing of GaAs and AlAs during the fabrication process, a simple cosine shaped corrugated interface is assumed, instead of the square-well shaped profile in the ideal case. The coordinate system is so chosen that z axis is vertical to the CLSSL with its upper interface corrugated along x direction. The geometry of the model is determined by the average width L_z of the CLSSL, the amplitude δL_z and lateral period L_x of its corrugated interface.

The calculation is carried out with the method we developed previously[16]. In the effective mass approximation, the eigenvalue equation and boundary conditions of an exciton are obtained by requiring the first-order difference of the following functional $L[\Psi]$ equal to zero ($\delta L = 0$), with

$$\begin{aligned} L[\Psi] &= \int \left\{ \frac{\hbar^2}{2m_e} \left[\left|\frac{\partial \Psi}{\partial x_e}\right|^2 + \left|\frac{\partial \Psi}{\partial y_e}\right|^2 + \left|\frac{\partial \Psi}{\partial z_e}\right|^2 \right] \right. \\ &+ \left. \frac{\hbar^2}{2m_{h,\parallel}} \left[\left|\frac{\partial \Psi}{\partial x_h}\right|^2 + \left|\frac{\partial \Psi}{\partial y_h}\right|^2 \right] + \frac{\hbar^2}{2m_{h,\perp}} \left|\frac{\partial \Psi}{\partial z_h}\right|^2 \right\} d\mathbf{r}_e d\mathbf{r}_h \\ &+ \int \left\{ V_e(\mathbf{r}_e) + eFz_e + V_h(\mathbf{r}_h) - eFz_h - \frac{e^2}{\epsilon|\mathbf{r}_e - \mathbf{r}_h|} \right\} |\Psi(\mathbf{r}_e, \mathbf{r}_h)|^2 d\mathbf{r}_e d\mathbf{r}_h \\ &- (E_{ex} - E_g) \int |\Psi(\mathbf{r}_e, \mathbf{r}_h)|^2 d\mathbf{r}_e d\mathbf{r}_h \end{aligned} \tag{1}$$

where $m_{e(h),\|(\perp)}$ is the electron (hole) effective mass in the direction parallel (vertical) to the CLSSL, $V_{e(h)}(\mathbf{r}_{e(h)})$ is the electron (hole) band offset between bulk GaAs and AlAs, F is the vertically applied electric field, E_g is the band gap between the conduction and valence bands in bulk GaAs, and E_{ex} is the exciton energy to be determined. To overcome the calculation difficulty due to the complicated boundary conditions of the electron and hole on the corrugated interface of the CLSSL, we introduce the same coordinate transformation for the electron and hole coordinates as that in reference [16], which transforms the CLSSL into a QW with planar interfaces and the average well width of the CLSSL, plus effective lateral periodic potentials for the electron and hole due to the corrugated interface. When a constant electric field is applied vertically to the CLSSL, strictly speaking, no bound state exists if the barrier height of the CLSSL is finite. The electron and hole will finally tunnel out of the CLSSL. But the tunneling becomes negligible for CLSSLs with wide well widths ($L_z \approx 10nm$) and in intermediate electric fields ($|F| \approx 100kV/cm$), which we are interested. Quasi bound states exist in the CLSSLs. The exciton Stark effect in the CLSSL is analyzed by a perturbation method[18], where the effective potentials due to the corrugated interface and applied electric field are considered as perturbations of the Hamiltonian, while the exciton states of the CLSSL are expanded with the eigen-wave functions of the corresponding QW in the transformed space $\tilde{\mathbf{r}}_{e(h)}$:

$$\tilde{\Psi}_{\mathbf{k}}(\tilde{\mathbf{r}}_{\|}, \tilde{\mathbf{R}}_{\|}, \tilde{z}_e, \tilde{z}_h) = \sum_{l_1, l_2, m, \nu} A_{l_1, l_2, m, \nu}(\mathbf{k}) \zeta_{l_1}^{(e)}(\tilde{z}_e) \zeta_{l_2}^{(h)}(\tilde{z}_h) \frac{\exp[i(\mathbf{k}+\mathbf{Q}_m)\cdot \tilde{\mathbf{R}}_{\|}]}{\sqrt{L_x^{(0)} L_y^{(0)}}} \phi_\nu(\tilde{\mathbf{r}}_{\|}) \qquad (2)$$

where $\tilde{\mathbf{r}}_{\|} = \tilde{\mathbf{r}}_{e,\|} - \tilde{\mathbf{r}}_{h,\|}$ and $\tilde{\mathbf{R}}_{\|} = (m_e \tilde{\mathbf{r}}_{e,\|} + m_{h,\|}\tilde{\mathbf{r}}_{h,\|})/(m_e + m_{h,\|})$ are coordinates describing the internal and CM motion of the exciton parallel to the CLSSL in the transformed space $\tilde{\mathbf{r}}_{e(h)}$. $\zeta_{l_1}^{(e)}(\tilde{z}_e)$ $[\zeta_{l_2}^{(h)}(\tilde{z}_h)]$ is the electron (hole) eigen-wave function of the corresponding QW in space $\tilde{\mathbf{r}}_{e(h)}$. The in-plane wave vector $\mathbf{k}$ of the exciton is limited within the first Brillouin zone (FBZ) determined by the lateral period L_x of the CLSSL, $|k_x| \leq Q/2 = \pi/L_x$, with the reciprocal lattice wave vector $\mathbf{Q}_m = mQ\mathbf{i}$. $L_x^{(0)} L_y^{(0)}$ is the area of the CLSSL interface, with $L_x^{(0)} = N_x L_x$ ($N_x \rightarrow \infty$). The internal motion of the exciton parallel to the CLSSL can, in principle, be expanded with the eigen-wave functions $\phi_\nu(\tilde{\mathbf{r}}_{\|})$ of a 2D hydrogen atom. So far, the exciton wave function in eq.(2) is exact, as all the expansion functions form orthogonal complete sets. In our calculation, we approximate the exciton wave function by restricting ν to only $\nu = 0$, and assuming a variational wave function $\phi_0(\tilde{\mathbf{r}}_{\|}) = N_{\gamma_1,\gamma_2} \exp(-\gamma_1 \tilde{x}^2 - \gamma_2 \tilde{y}^2)$. It is possible to improve the accuracy by including more Gaussian expansion functions, if higher exciton energies (bands) are calculated. It should be noticed that the exciton wave function in eq.(2) gives the correct description of the CMQ of the exciton in the lateral direction. The lowest exciton energy (band) of the CLSSL in the electric field is obtained by diagonalizing the eigenvalue equation obtained by minimizing the functional $L[\Psi]^{16}$. A sufficient number of the expansion functions (l_1, l_2, m) is used in the numerical calculation so that the change of the calculated result is less than 1% if the number of the expansion functions is further increased. In the calculation, the discontinuity of the electron (hole) effective mass in the well and barrier materials is neglected for simplicity. The effective masses of the electron, heavy- and light-hole in the directions parallel and vertical to the GaAs/AlAs CLSSL are taken as $m_e = 0.067m_0$, $m_{hh,\parallel} = 0.103m_0$, $m_{hh,\perp} = 0.450m_0$, $m_{lh,\parallel} = 0.212m_0$ and $m_{lh,\perp} = 0.082m_0$. The electron (hole) band offset between the GaAs well and AlAs barrier is assumed to be $\Delta V_e = 1.06eV$ $(\Delta V_h = 0.53eV)$. The average dielectric constant is $\epsilon = 11.5$. And the conduction-valence band gap of GaAs is $E_g = 1.52eV$.

3. Results:

In fig.1, we give (a) the calculated exciton energy $E_{ex} - E_g$ (the solid lines) and (b) binding energy E_b (the solid lines) of the heavy- and light-exciton in a GaAs/AlAs CLSSL as functions of the applied electric fields. The structural parameters of the CLSSL are $L_z = 10nm$, $\delta L_z = 3nm$ and $L_x = 20nm$. Also given in fig.1 are the exciton and binding energies (the dashed lines) calculated for a GaAs/AlAs QW with a well width $L_z = 10nm$ in the same electric fields. It is interesting to note that the corrugated interface in the CLSSL causes a blue shift for the exciton energy of the heavy-exciton comparing with that in the unmodulated QW, while a red shift is predicted in the exciton energy of the light-exciton [fig.1 (a)]. Our result is different from that obtained by Glutsch and Bechstedt[14], where only the blue shift of the exciton energy was predicted. In their calculation, the anisotropy of the hole effective mass was neglected and the effect of the corrugated interface of the system was smeared out by taking an average in the vertical direction of the system. These two effects are important in explaining the result we obtained above. In the CLSSL, the electron and hole are attracted to the parts of the CLSSL where the width is wide. For the internal motion, the exciton "feels" a wider QW, which reduces the exciton energy corresponding to its internal motion. On the other hand, the periodic corrugated interface of the CLSSL introduces the CMQ, which for exciton states at the center of the FBZ ($\mathbf{k} = 0$), will increase the exciton energy corresponding to its CM motion. The increased energy is *inversely* proportional to the exciton CM, $M_\parallel = m_e + m_{h,\parallel}$, in the parallel direction[19]. These two effects compete to determine whether the exciton energy is blue or red shifted comparing with that of the unmodulated QW. For the excitons in the GaAs/AlAs CLSSL, the parallel CM of the light-exciton $M_{l,\parallel}$ is heavier than that of the heavy-exciton $M_{h,\parallel}$. So the energy increase, due to the CMQ, is smaller for the light-exciton which results in the red shift of its energy.

To investigate this effect in detail, we give in fig.2 (a) the calculated heavy-exciton energy $E_{ex} - E_g$ and (b) its Stark shift $E_{ex}(F) - E_{ex}(0)$ in the same CLSSL as that in fig.1 with different parallel hole effective masses $m_{hh,\parallel} = 0.103m_0$ (the solid line), $m_{hh,\parallel} = 0.2m_0$ (the dashed line), and $m_{hh,\parallel} = 0.06m_0$ (the dash-dotted line). Also given in fig.2 are the exciton energy and its Stark shift calculated for a GaAs/AlAs QW with a well width $L_z = 10nm$ and the same $m_{hh,\parallel}$ parameters. Actually, different parallel heavy hole effective masses, ranging from $m_{hh,\parallel} = 0.21m_0$ to $m_{hh,\parallel} = 0.027m_0$, have been used in the calculation of the excitons in GaAs CLSSLs and quantum wires.[15,20] Here we are not judging which value is more accurate. The results in fig.2 just show that it is possible to have red shifts in the heavy-exciton energy if $m_{hh,\parallel}$ becomes heavier. Due to the effect of the CMQ, the exciton energy and its Stark shift depend sensitively on $m_{hh,\parallel}$. While in QWs, especially the exciton Stark shift is almost independent of $m_{hh,\parallel}$.

In fig.3, we give the calculated heavy- and light-exciton energies $E_{ex} - E_g$ in different electric fields as functions of the lateral period L_x of the same CLSSL as that in fig.1. As $L_x \to \infty$, the exciton energies approach those of a GaAs/AlAs QW with a well width $L_z = 13nm$, indicated by the black squares and circles.

In QWs, the exciton motion of its CM in the parallel direction is separated from the internal motion of the excitons. The total exciton energy forms a parabolic band

$$E_{ex}^{(n)}(\mathrm{k}) = E_{ex}^{(n)} + \frac{\hbar^2 k^2}{2M_\parallel}$$

where the second term gives the exciton energy corresponding to its CM motion. When the periodic corrugated interface is present in the CLSSL, apart from changing the exciton energy corresponding to its internal motion, it also breaks the parabolic band into mini-bands at $k_x = (1/2 + m)Q$ (CMQ). For the lowest exciton energy mini-band, the CMQ flattens the band by increasing the exciton energy at the centre of the FBZ and decreasing the energy at the edge of the FBZ. In fig.4, we give the calculated lowest exciton energy mini-band, $E_{ex}(k_x) - E_{ex}(0)$, (the solid lines) in the same CLSSL as that in fig.1. Also given in fig.4 are the exciton energy band (the dashed lines) calculated for a GaAs/AlAs QW with a well width $L_z = 10nm$. The effect of the band-flattening caused by the CMQ is obvious. The exciton mini-bands induced by the CMQ were also reported in the work by Glutsch and Bechstedt.

The effect of the CMQ not only introduces the exciton mini-bands, it also changes the distribution of the exciton. We define the probability distribution of the exciton CM in the CLSSL in the original space $\mathbf{r}$ by:

$$P(X) = \int dz_e dz_h \, |\Psi_{\mathbf{k}}(x, X, z_e, z_h)|^2_{x=0} \tag{3}$$

It is easy to show that $P(X + L_x) = P(X)$. In fig.5, we plot $P(X)$ for (a) the heavy- and (b) light-exciton in the same CLSSL as that in fig.1. The light-exciton in the CLSSL is more localized in the distribution than the heavy-exciton due to its heavier parallel CM.

Conclusions: The QCSE of the excitons in the GaAs/AlAs CLSSLs is calculated with the method we developed previously, which overcomes the difficulty due to the complicated boundary conditions of the electron and hole on the non-planar interfaces of the CLSSLs. The blue and red shifts in the exciton energies are predicted for the heavy- and light-excitons in the CLSSLs, respectively, comparing with those in the unmodulated QW due to the different effective hole masses in the parallel direction. To obtain the correct QCSE of the excitons in the CLSSLs, an accurate determination of the hole effective mass $m_{h,\|}$ in the parallel direction is necessary, since the QCSE becomes sensitively dependent on $m_{h,\|}$ because of the CMQ. The CMQ also causes the flattening of the exciton mini-bands and the localization of the excitons in the parts of the CLSSLs where the well width is wide.

Acknowledgments: This work is supported by the National Natural Science Foundation of China, the Pan-Deng Program of the Chinese National Committee of Science and the Direct Grant for Research of the Chinese University of Hong Kong under contract No. 2060137. The author is grateful to Prof. K.W. Yu for the instructive discussions on the subject and hospitality received during his stay in the Chinese University of Hong Kong. The author would also like to thank the Abdus Salam International Centre for Theoretical Physics, Trieste, for hospitality during his visit there.

References

1. D.A.B. Miller, D.S. Chemla, T.C. Damen, A.C. Gossard, W. Wiegmann, T.H. Wood, and C.A. Burrus, *Phys. Rev. Lett.* **53**, 2173 (1984).
2. C. Fan, D.W. Shih, M.W. Hansen, S.C. Esener, and H.H. Wieder, *IEEE Photonics Technology Lett.* **5**, 1383 (1993).
3. X.B. Mei, K.K. Loi, H.H. Wieder, W.S.C. Chang, and C.W. Tu, *Appl. Phys. Lett.* **68**, 90 (1996).
4. L.M. Zhang and J.E. Carroll, *IEEE J. Quantum Electron. QE* **30**, 2573 (1994).
5. Y.M. Huang and C.H. Lien, *J. Appl. Phys.* **78**, 2700 (1995).
6. P.J. Thompson, S.Y. Wang, G. Horsburgh, T.A. Steele, K.A. Prior, and B.C. Cavenett, *Appl. Phys. Lett.* **68**, 946 (1996).
7. A.A. Toropov, T.V. Shubina, S.V. Ivanov, A.V. Lebedev, S.V. Sorokin, E.S. Oh, H.S. Park, and P.S. Kopev, *J. Cryst. Growth* **159**, 463 (1996).
8. S.W. Short, S.H. Xin, A. Yin. H. Lou, M. Dobrowolska, and J.K. Furdyna, *J. Electronic Materials* **25**, 253 (1996).
9. A. Sa'ar, A. Givant, S. Calderon, O. Benshalom, E. Kapon, A. Gustafsson, D. Oberli, and C. Caneau, *Supperlatt. Microstruct.* **19**, 217 (1996).
10. S. Jaziri, G. Bastard, and R. Bennaceur, *J. de Physique IV* **3**, 367 (1993).
11. M. Tsuchiya, J.M. Gaines, R.H. Yan, R.J. Simes, P.O. Holtz, L.A. Coldren, and P.M. Petroff, *Phys. Rev. Lett.* **62**, 466 (1989).
12. R. Nötzel, N.N. Ledentsov, L. Däweritz, M. Hohensten, and K. Ploog, *Phys. Rev. Lett.* **67**, 3812 (1991).
13. H. Akiyama, T. Someya, and H. Sakaki, *Phys. Rev. B* **53**, R4229 (1996).
14. S. Glutsch and F. Bechstedt, *Phys. Rev. B* **47**, 6385 (1993).
15. J.B. Xia and S.S. Li, *Phys. Rev. B* **51**, 17203 (1995).
16. H. Sun, J.M. Huang, and K.W. Yu, *J. Phys.: Condens. Matter* **8**, 7605 (1996).
17. S. Huant, M. Fischer, and B. Etienne, *Solid State Commun.* **104**, 183 (1997).
18. G. Lengyel, K.W. Jelley, and R.W.H. Engelmann, *IEEE J. Quantum Electron. QE* **26**, 296 (1990).
19. C. Kittel, *Introduction to Solid State Physics*, (John Wiley & Sons, New York, 1961), second edition, p. 279.
20. F.L. Madarasz, F. Szmulowicz, and F.K. Hopkins, *Phys. Rev. B* **52**, 8964 (1995).

Figure Captions

Fig.1 (a) the calculated exciton energy $E_{ex} - E_g$ (the solid lines) and (b) the binding energy E_b (the solid lines) of the heavy- and light-excitons in a GaAs/AlAs CLSSL as functions of the applied electric fields for the lowest exciton states with $\mathbf{k} = 0$. The structural parameters of the CLSSL are $L_z = 10nm$, $\delta L_z = 3nm$ and $L_x = 20nm$. Also given in fig.1 are the exciton and binding energies (the dashed lines) calculated for a GaAs/AlAs QW with a well width $L_z = 10nm$ in the same electric fields.

Fig.2 (a) the calculated heavy-exciton energy $E_{ex} - E_g$ and (b) its Stark shift $E_{ex}(F) - E_{ex}(0)$ in the same CLSSL as that in fig.1 for the lowest exciton states ($\mathbf{k} = 0$), with different parallel hole effective masses $m_{hh,\|} = 0.103m_0$ (the solid line), $m_{hh,\|} = 0.2m_0$ (the dashed line), and $m_{hh,\|} = 0.06m_0$ (the dash-dotted line). Also given in fig.2 are the exciton energy and its Stark shift calculated for a GaAs/AlAs QW with a well width $L_z = 10nm$ and the same $m_{hh,\|}$ parameters.

Fig.3 The calculated heavy- and light-exciton energies $E_{ex} - E_g$ in different electric fields as functions of the lateral period L_x of the same CLSSL as that in fig.1 for the lowest exciton states ($\mathbf{k} = 0$). The black squares and circles are the heavy- and light-exciton energies of a GaAs/AlAs QW with a well width $L_z = 13nm$ in the same electric fields.

Fig.4 The calculated lowest exciton energy mini-band $E_{ex}(k_x) - E_{ex}(0)$ (the solid lines) as functions of the reduced in-plane wave vector k_x/Q in the same CLSSL as that in fig.1. Also given in fig.4 are the exciton energy band (the dashed lines) calculated for a GaAs/AlAs QW with a well width $L_z = 10nm$.

Fig.5 The probability distribution of (a) the heavy- and (b) light-exciton CM in the same CLSSL as that in fig.1, as functions of the reduced CM position X/L_x.

Fig.1 (a)

Exciton energy in CLSSLs in electric fields

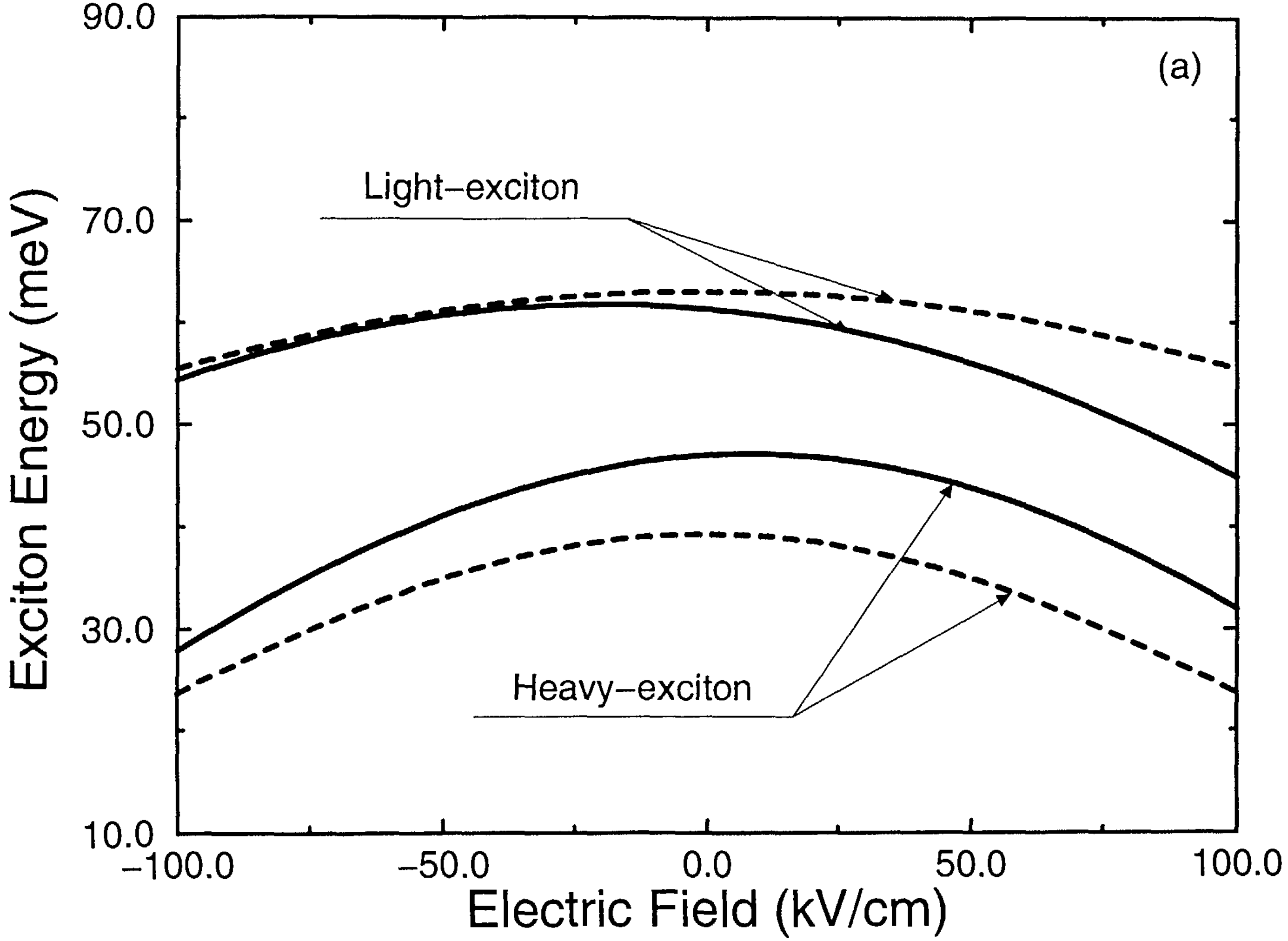

Fig.1 (b)

Binding energy in CLSSLs in electric fields

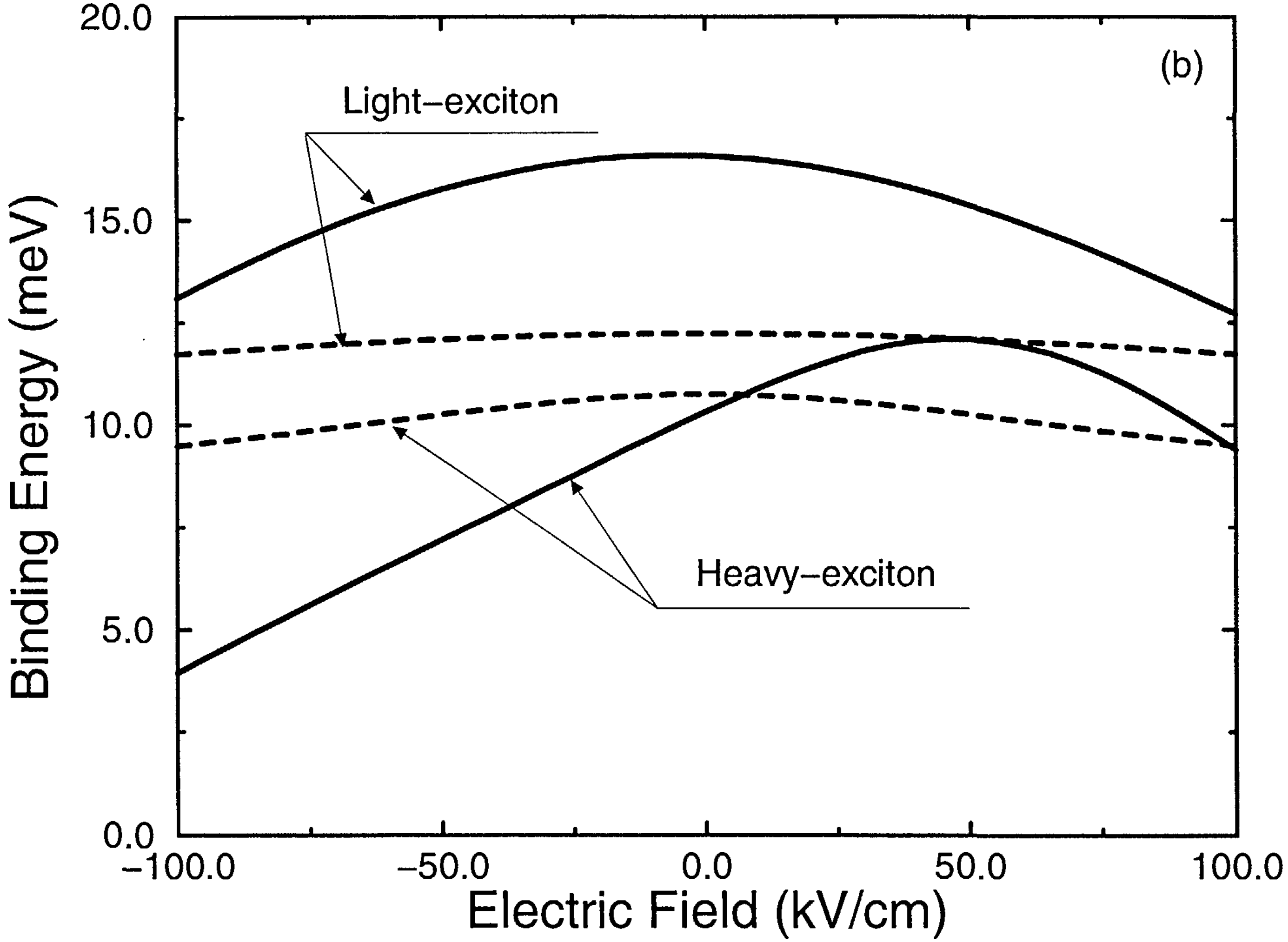

Fig.2 (a)

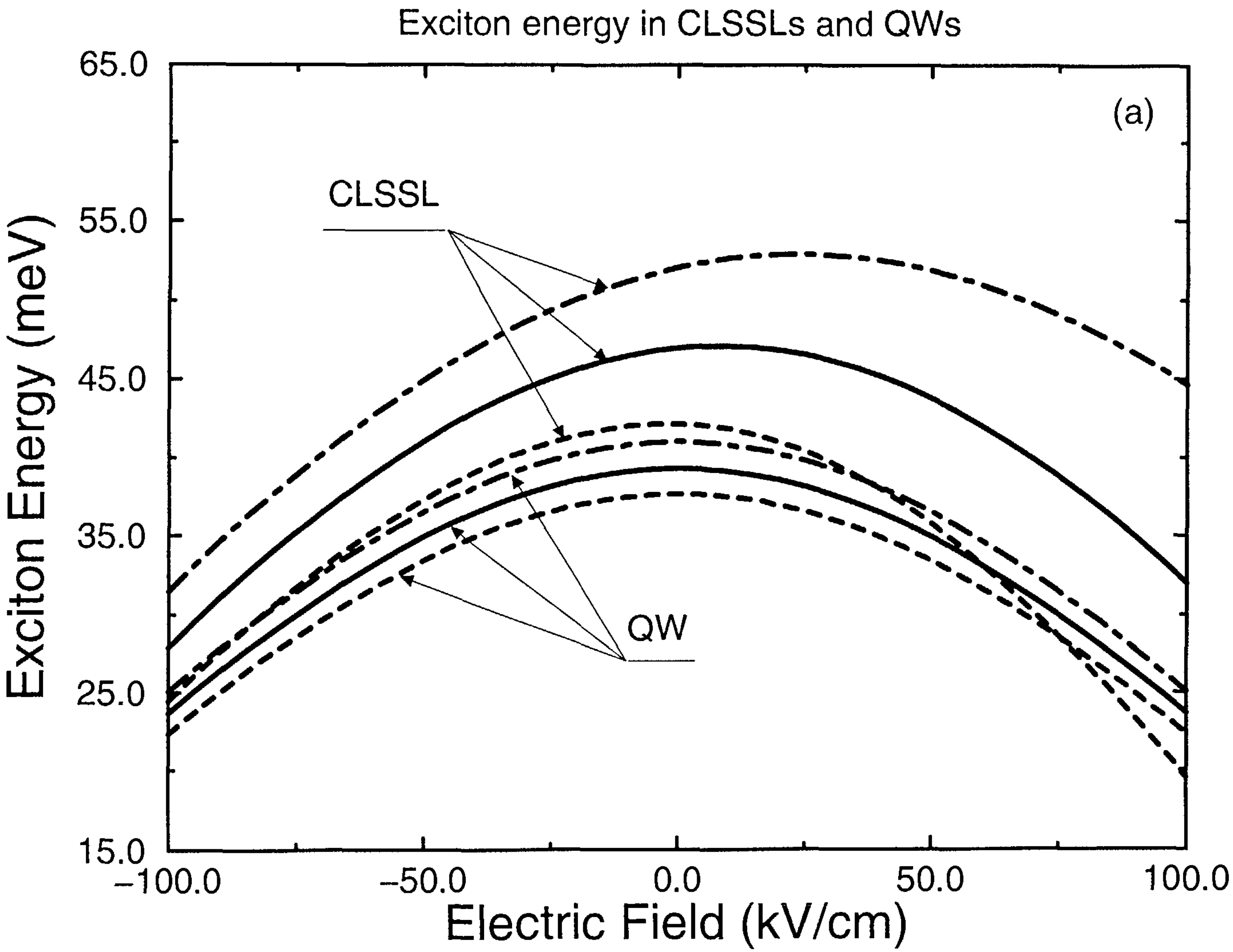

Exciton energy in CLSSLs and QWs
(a)
CLSSL
QW
Exciton Energy (meV)
Electric Field (kV/cm)
65.0
55.0
45.0
35.0
25.0
15.0
−100.0
−50.0
0.0
50.0
100.0

fig.2 (b)

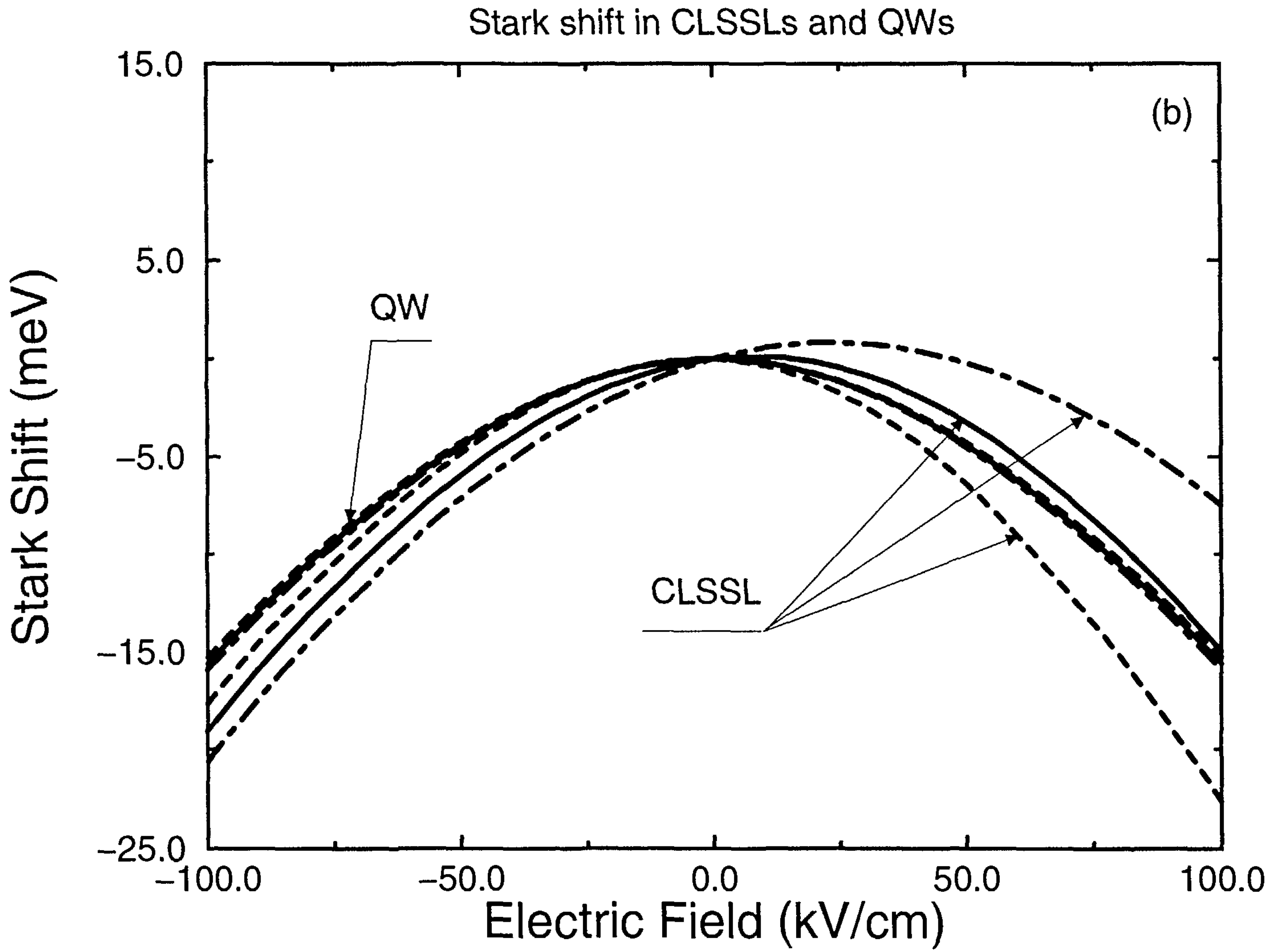
Stark shift in CLSSLs and QWs
(b)
QW
CLSSL
15.0
5.0
−5.0
−15.0
−25.0
−100.0
−50.0
0.0
50.0
100.0
Stark Shift (meV)
Electric Field (kV/cm)

Fig.3

Exciton energy as function of lateral period

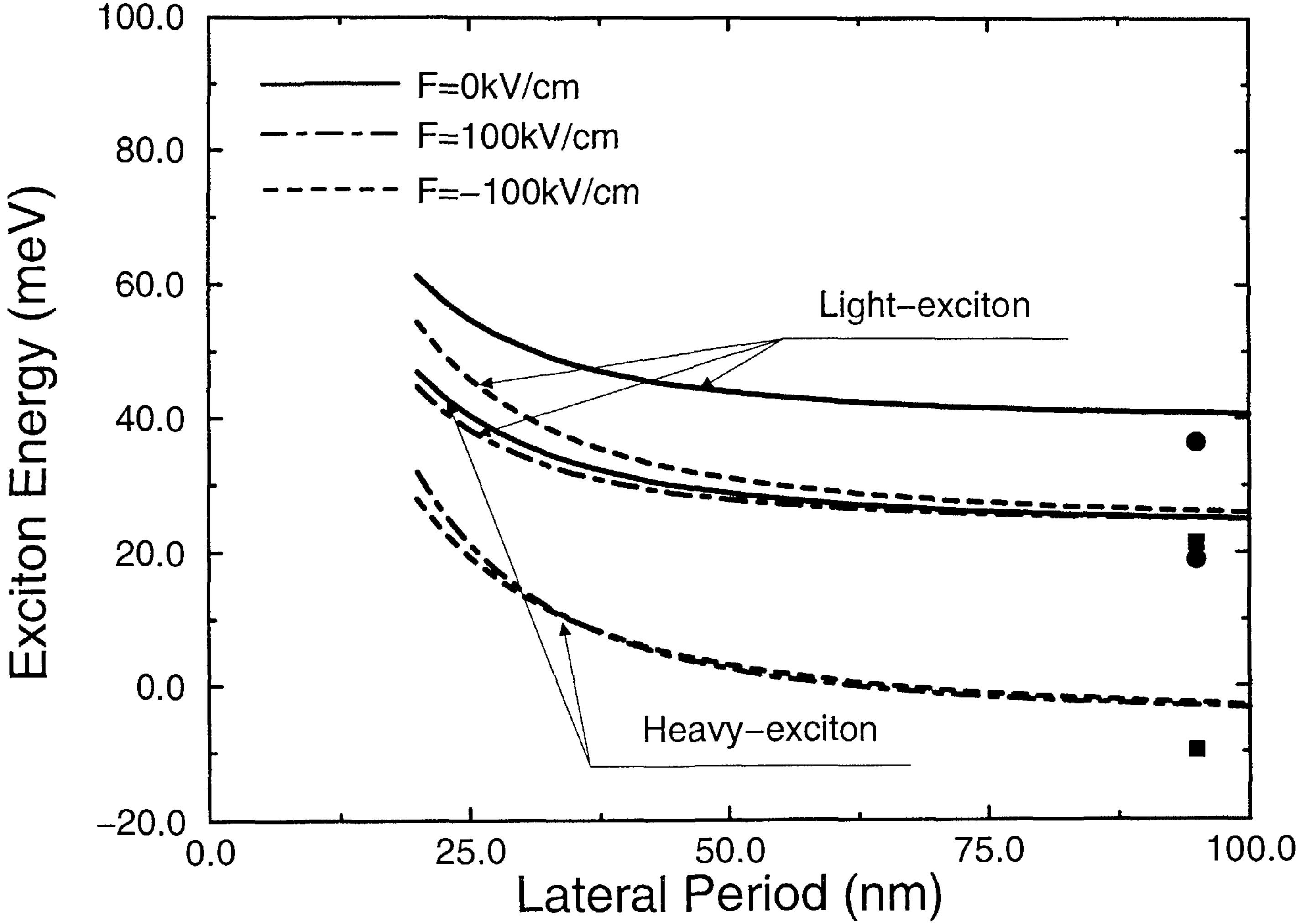

Fig.4

Exciton band in CLSSLs and QWs

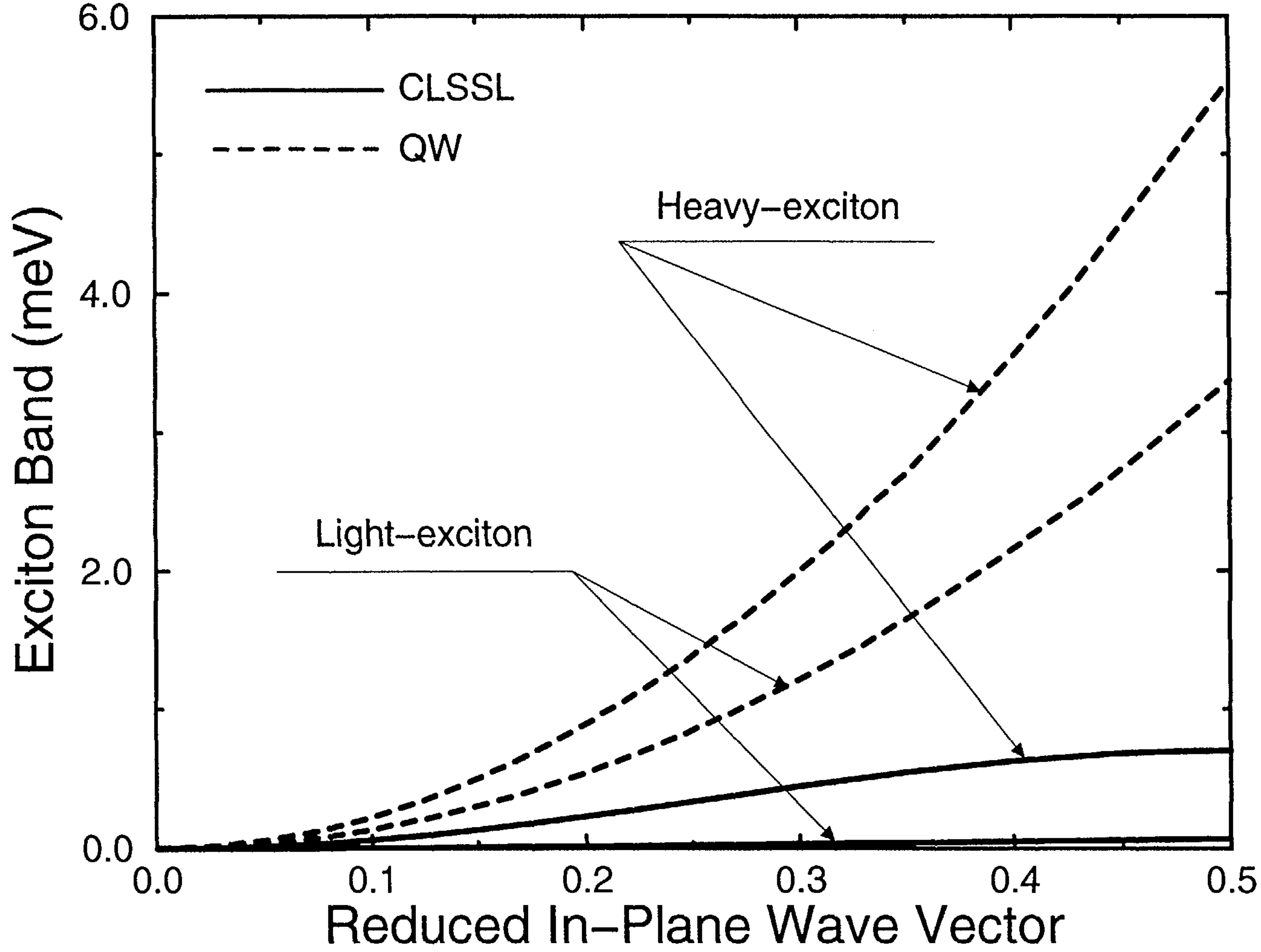

Fig.5 (a)

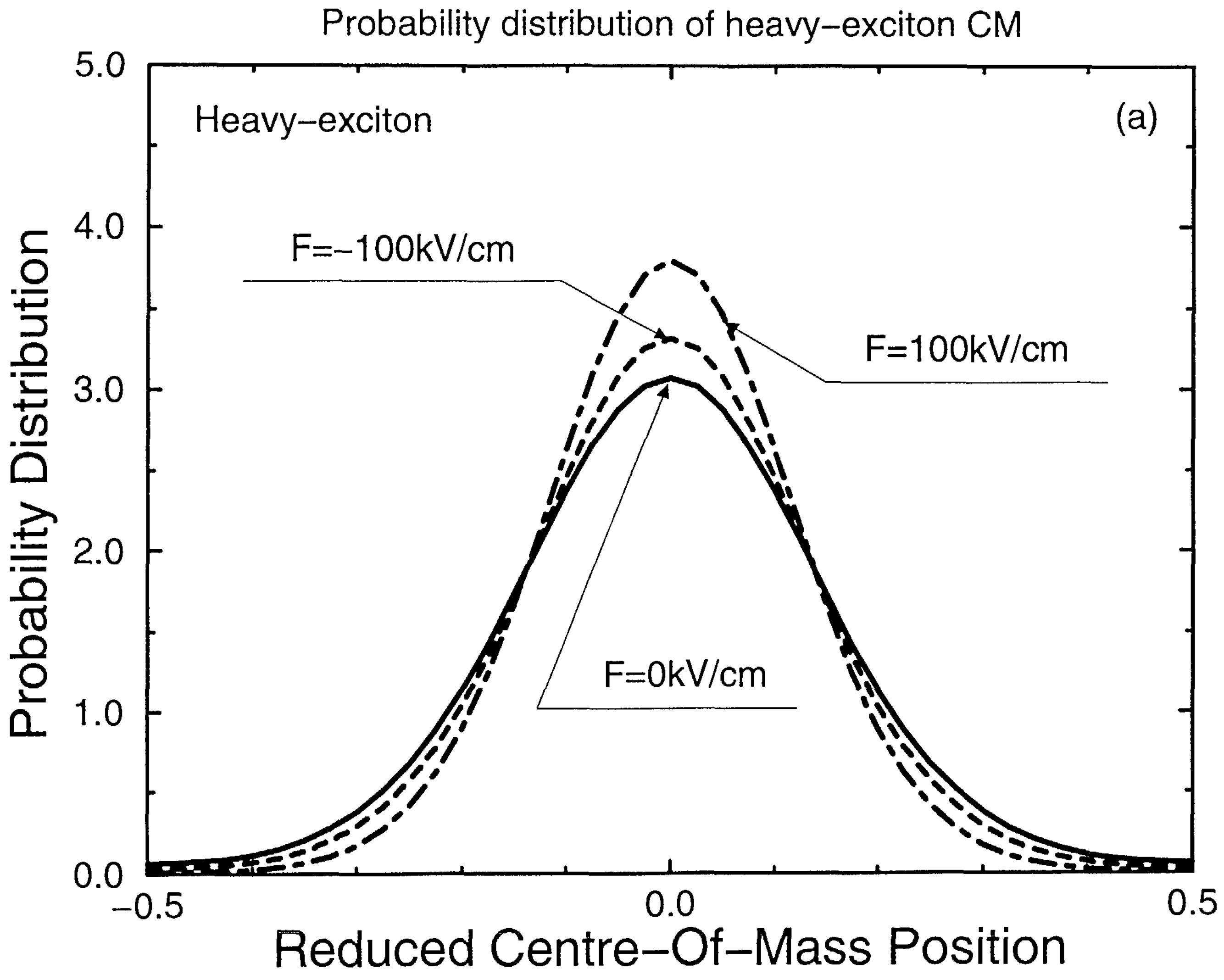
Probability distribution of heavy-exciton CM
Heavy-exciton
(a)
F=-100kV/cm
F=100kV/cm
F=0kV/cm
Probability Distribution
Reduced Centre-Of-Mass Position
5.0
4.0
3.0
2.0
1.0
0.0
-0.5
0.0
0.5

Fig.5 (b)

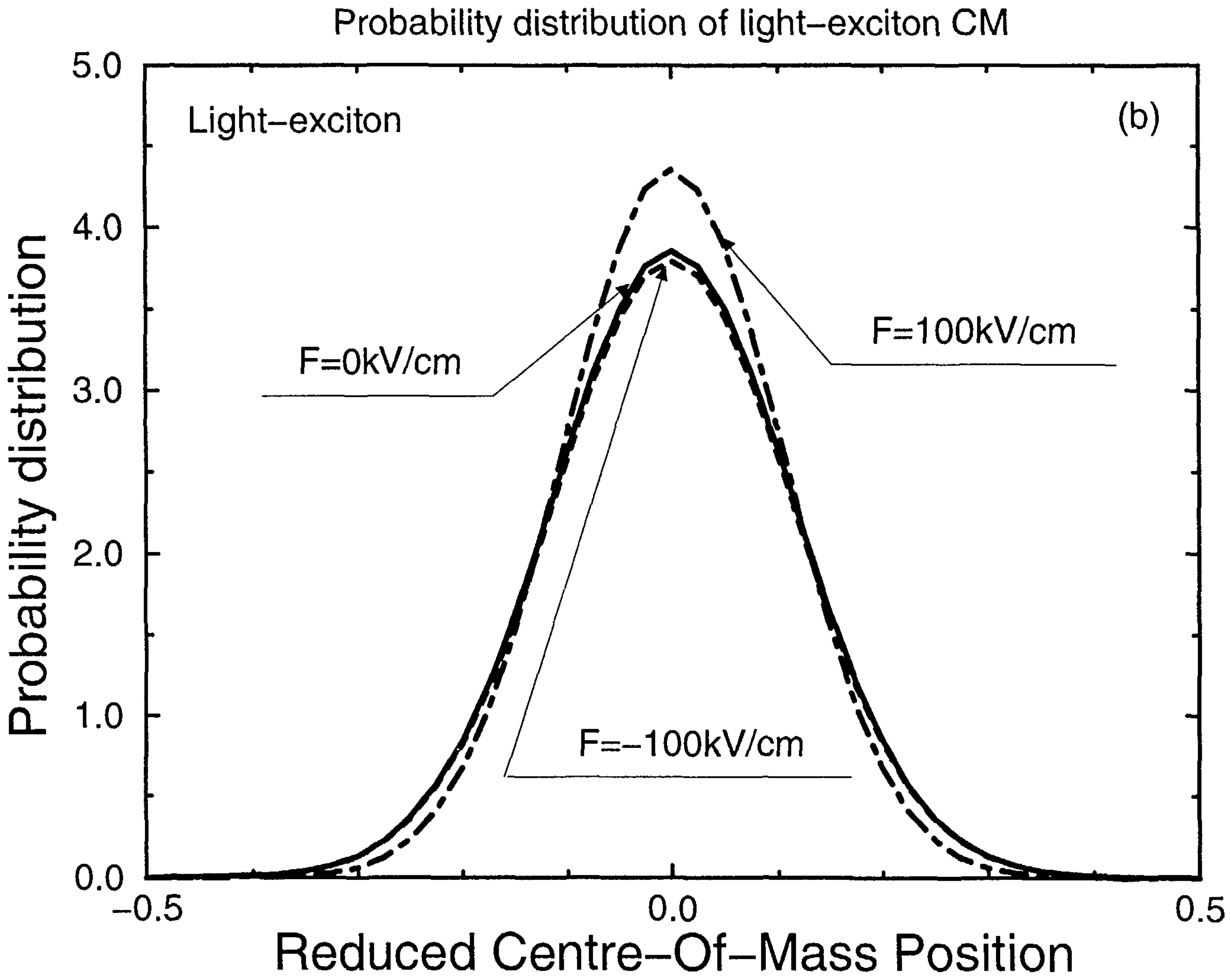
Probability distribution of light−exciton CM
Light−exciton
(b)
F=0kV/cm
F=100kV/cm
F=−100kV/cm
Probability distribution
Reduced Centre−Of−Mass Position
5.0
4.0
3.0
2.0
1.0
0.0
−0.5
0.0
0.5